NATIONAL AERONAUTICS AND SPACE ADMINISTRATION

Technical Report 32-1443

Analysis of Surveyor Data

JET PROPULSION LABORATORY
CALIFORNIA INSTITUTE OF TECHNOLOGY
PASADENA, CALIFORNIA

June 30, 1969

Photometry and Polarimetry of the Earth

J. J. Rennilson
California Institute of Technology
Pasadena, California

H. H. Holt
U. S. Geological Survey
Flagstaff, Arizona

I. Introduction

During the *Surveyor VII* mission, the earth was easily visible in the narrow-angle mode of the television camera. The objectives of observing the earth were twofold: to measure the average luminance of the earth over as great a range of phase angles as possible, and to measure the degree and orientation of the polarization of light reflected from the earth. Each of these objectives was new, as the only complete previously existent data on the photometric and polarimetric properties of the earth were derived by indirect astronomical measurements of the moon.

This paper summarizes the results, thus far, of these measurements and does not attempt to explain or correlate the data with other factors, such as geographic location, weather conditions, etc.

II. Observing Conditions

The landed site of *Surveyor VII* at 11.47 deg W and 40.86 deg S positioned the earth at camera elevations ranging from 45 to 55 deg during the lunar day. Figure 1 shows the variation of phase angle of the earth with the terrestrial date during the mission. The circles on the figure indicate the times when camera exposures were made of the earth. The last two days of the mission were devoted to observations made on the average of once every two hours.

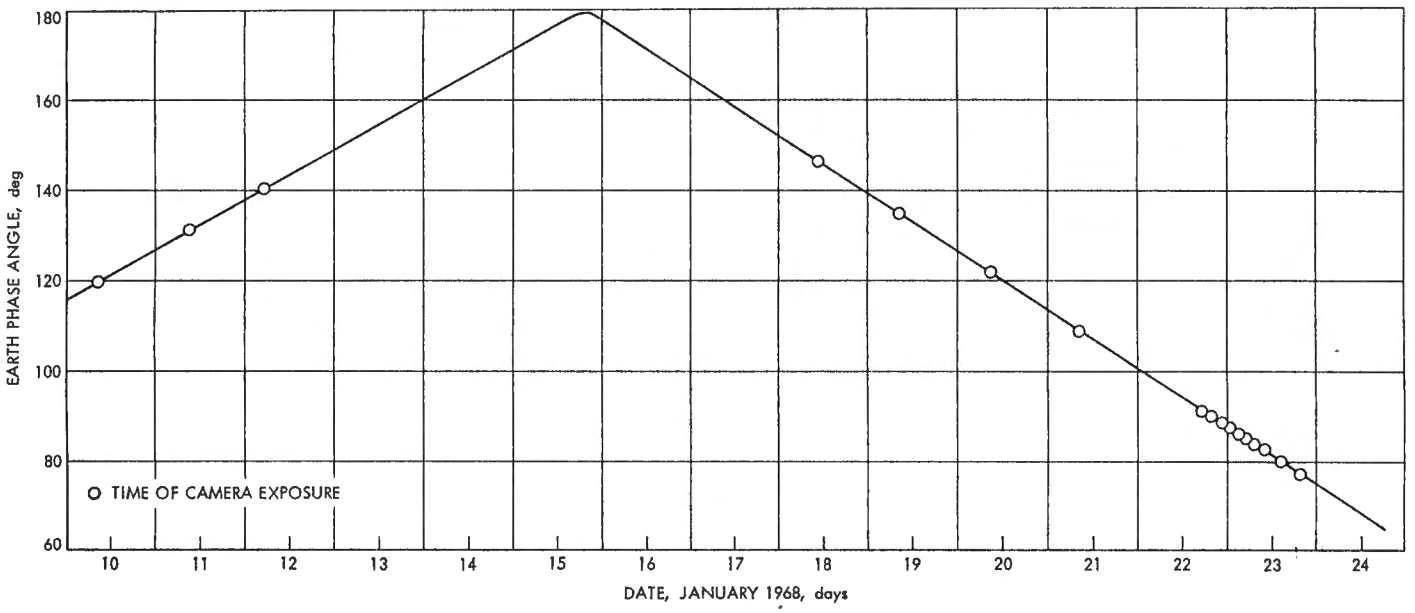

Fig. 1. Plot of phase angle of earth as seen from the *Surveyor VII* site

The general procedure in making these measurements was to expose the camera to the earth luminance such that the brightest portions would register a video signal just below the saturation level. A series of two frames each was then taken through each of the four filter positions. The camera was then opened one full iris setting; the above procedure was repeated. By using this technique, the entire range of earth luminances was measured by a camera response of more limited exposure latitude.

Close to the actual times of earth observation, a measurement was made of one of the three illuminated photometric targets on the spacecraft. The preflight calibration values for absolute luminance could be thus verified.

A total of 823 frames were taken of the earth during the lunar day. Not all of these frames were taken for photometric and polarimetric purposes. From the total number only 135 frames were selected for computer processing. The results given in this paper are the first reduction of these observations (Ref. 1).

III. Camera Parameters

A. Polarizing Filters

The *Surveyor VII* camera was equipped with an accurate position filter wheel so that the measurement with polarizing filters would be precise. The polarizing filters on this camera were formed of glass laminated, linearly polarizing dichroic (KN-36) material, 3 mm thick. The filters were cut such that their transmission axes were oriented at angles of 0, 45, and 90 deg when they were rotated into the light path. The 0-deg orientation was parallel to the mirror surface and perpendicular to the plane containing the mirror normal and the camera optical axis. The filter wheel, and thus the polarizing filters, are an integral part of the mirror housing and rotate with it. The fourth position on the wheel was a piece of clear glass with a coating of inconel of sufficient density so that the transmission of the glass was equal to that of the polarizing filters.

The exact position of the transmission axes of the filters with respect to the mirror assembly was determined in preflight calibration. A polarizing filter of the same type was mounted in a graduated rotating cell before the light source. The light source was positioned along the tilt axis of the camera. Thus, the mirror elevation axis and an exact 0-deg transmission axis of the first polarizing filter would be horizontal. The polarizing filter was then rotated until extinction, which was marked by a minimum camera signal, occurred. The angle was then read and the corresponding orientation of the polarizing filter in the filter wheel was then determined. This method was repeated for each filter position.

The measurement of the polarization of earth light was further complicated in the *Surveyor VII* camera by

the viewing mirror. The polarized earth light undergoes an alteration of type and orientation after reflection by the metallic mirror. In general, linearly polarized light incident on an overcoated aluminized mirror will be transformed into elliptical polarization. Measurement of this polarization by three linear analyzers will result in erroneous values dependent on the amount of elliptical polarization.

Figure 2 shows the effect of a metallic mirror on linear polarization at varying angles of incidence. For observation of the lunar surface especially close to the spacecraft at $i = 25$ deg (camera elevation -40 deg), the effect is not too serious. For the earth observation, however, incidence angles of 65–70 deg are the rule, and mirror effect is very important.

One method of eliminating this source of error is to measure the property of the mirror to alter the linear polarized light. Known amounts and orientations of linear polarized light are made incident on the mirror at various incident angles. The resultant elliptical polarization is then measured.

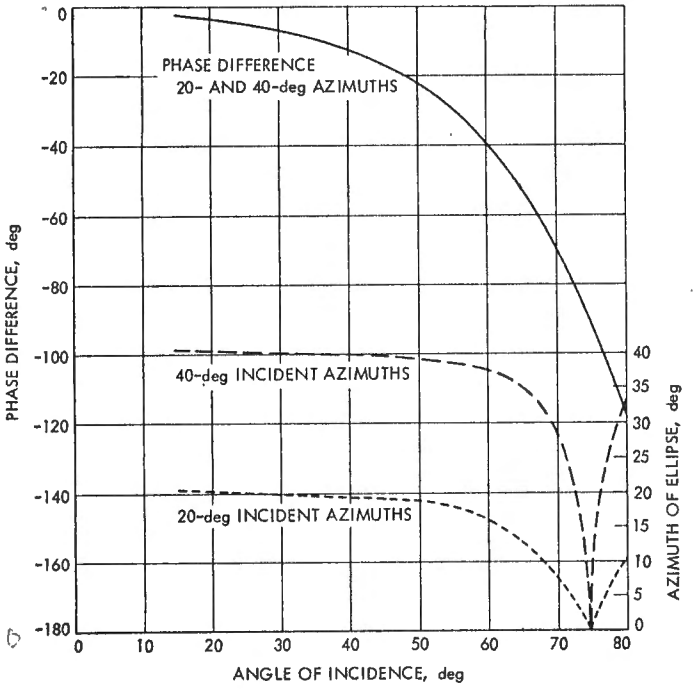

Fig. 2. Plot of elliptical polarization resulting from incident linear polarized light incident on a *Surveyor* mirror (phase difference is plotted against angle of incidence for azimuths of incident linear polarization of 20 and 40 deg; azimuth of incident light is measured from plane of mirror counter-clockwise; and azimuth angle of ellipse is also shown for 20 and 40 deg)

The capability of a metallic mirror to alter the polarization form of incident light may be described mathematically by a 4×4 matrix of coefficients, known as the Mueller matrix. A four-component vector, called the Stokes vector, completely describes any form of polarization. Thus, the resultant polarization form of reflected light specified by a Stokes vector can be calculated by premultiplying the incident polarized light (Stokes vector) by the Mueller matrix of the mirror. Thus,

$$S' = MS$$

The incident Stokes vector is then given by the equation $S = M^{-1} S'$.

In measuring partially polarized light using only three linear polarizing filters, the complete Stokes vector (which includes phase information) cannot be determined. Thus, an assumption must be made concerning the type of incident polarized light; e.g., that it is linear. In the case of the lunar surface, this is probably a reasonable assumption; however, it may be somewhat in doubt when applied to the earth. In this paper, however, only linear polarization is assumed.

B. Photometry

Photometric measurements of the earth were taken through the clear filter position, thus using the entire camera spectral response. Hence, the measurements would not be correct unless the spectral distribution of the scene closely corresponded with that used during calibration. Fortunately, the spectral power distribution of sunlight reflected from clouds was very similar to that of sunlight above the atmosphere. The light sources used to calibrate the television camera before flight possessed spectral power distributions very similar to the sun. Exact correction factors for even the slight deviation between the sunlight and these sources were determined for *Surveyor VII*.

For the clear position, the luminances have a correction factor of 1.17 and have been corrected for this paper. The parts of the earth, such as the oceans and continents, having different distributions must of necessity have larger correction factors. However, for this

paper, they were not estimated because of the large dominance of the cloud cover.

IV. Data Reduction

The computer processing of the selected earth frames follows the flow diagram outlined in Fig. 3. After selection of the most important frames (flight pictures), processing begins with analog to digital conversion.

The composite video signal is recorded during the mission on magnetic tape simultaneously with the photographic image. This composite signal consists of all associated data, such as horizontal and vertical synchronization pulses, camera parameters given in a pulse code, and video frame. The signal is recorded in the frequency domain.

The analog tape then is replayed at a reduced speed (from 60 to 7½ ips) and passed through a 30-kHz filter to a demodulator. The demodulator converts the composite video to voltages. The voltages are converted to digital values scaled at 8 bits. The most significant 6 bits are then recorded on digital magnetic tape. Digitized black is given the value of 63, and white of 00. The digital values are then rearranged in the computer, line by line, until a picture frame of 600 lines is complete. Each line is broken into 684 elements rather than the normal 600 elements in order to utilize more of the densely packed information (frequency) along a line. Thus, a

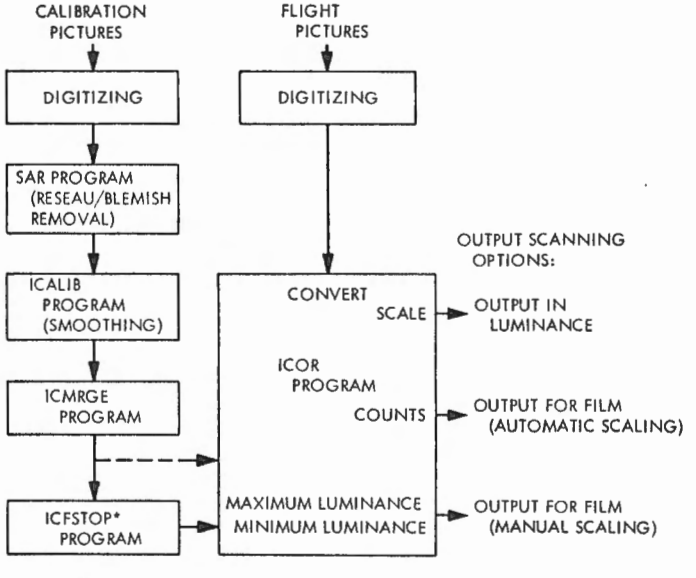

*NOT REQUIRED IF CALIBRATION AND FLIGHT PICTURES ARE AT SAME f-STOP.

Fig. 3. Computer processing flow diagram

digitized frame consists of 600 × 684 picture elements (or pixels as they are called).

Referring to the flow diagram, the processing continues with the digitization of the calibration pictures. These frames, taken at increasing luminance levels, are chosen to allow close interpolation of the light-transfer characteristics. Removal of reseau and blemishes is then applied. The ICALIB program smoothes the data by an averaging routine and eliminates effects of periodic noise. The resulting smoothed frames are then combined into calibration data set, using the ICMRGE program. For a given digital value, the scaled luminance is calculated from this data set.

The *Surveyor* cameras have shown a variation of transfer characteristics that is dependent on the iris and requires the actual monitoring by a potentiometer.

The frame position, as well as the signal amplitude, requires that an interpolated data set be made between calibration data sets used at the same iris setting as the flight frame. The large number of frames taken on the lunar surface were not taken at the iris positions that the preflight pictures were. The program that generates the interpolated data set is ICFSTOP.

The final processing uses a program called ICOR to compute the scaled luminances from the digitized flight picture, using the ICFSTOP data set at the same iris position. Scaled luminances are obtained by adjusting the output so that the maximum luminance is less than the product of the scaling factor and 255 (8 bits). All frames included in this reduction have been processed in this manner.

To check the absolute luminances, a measurement of the photometric targets was made during the mission. These frames were processed in the same manner as the earth pictures, and the resultant luminances were plotted against assumed values determined from preflight goniophotometric calibration of the targets. Correction to these assumed values was made for spacecraft reflection. Luminances determined by this technique are believed to be within an accuracy of $\pm 10\%$.

V. Photometric Results

The average earth luminance was obtained by summing the pixel luminances and dividing by the number

of elements. Certain judgment was required as to the geometrical limit of the image, especially along the terminator; however, the results are believed well within the measurement error.

The plot of the average earth luminance as a function of phase angle is given in Fig. 4. The black dots represent the values before conjunction. The spread of the luminances is due to meteorological conditions. For comparison, the curves obtained previously by astronomical observation (Ref. 2) of earthshine on the moon are also included in the figure. The ρ symbol is the Bond albedo or the reflectance in the new photometric terminology defined by the CIE (Commission Internationale d'Eclairage) standard. The specular peak appears to start earlier than previously measured, and all the values are higher than that observed.

The value of earthshine at the lunar surface was calculated from these average luminances. For this purpose, the solid angle was calculated using the equation:

$$E = \pi L \tau \sin^2 \theta$$

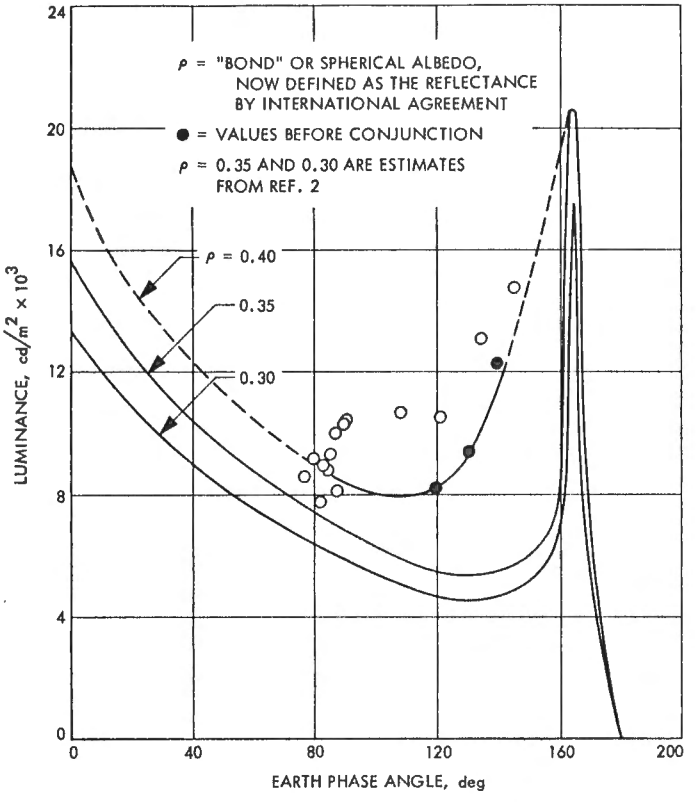

Fig. 4. Plot of average earth luminance as a function of phase angle

where L is the average earth luminance, τ is the fraction of the disk illuminated by sunlight, and θ is the angular semidiameter of the earth on the date of observation. The average earth illuminance normal to the surface is given in Fig. 5.

VI. Polarimetric Results

The images of the earth (Figs. III-95 and III-96 of Ref. 1) show a prominent patch of light on the spheroid that is directly associated with specular reflection of sunlight from the oceans. This reflection, as is the sun glint off the surface of a lake or pond, is heavily polarized. The polarization of this patch of light amounts to 32% as measured on one image of the earth.

Polarization measurements of similar areas on the remaining earth frames are in progress. It is expected that the specularly reflected sunlight will be the predominant factor in the integrated polarimetric function of the earth.

The orientation of polarization is perpendicular to the phase plane. The phase plane is being defined as the plane formed by the vectors from the earth center to the center of the moon and sun, respectively.

It is interesting to note that the degree of polarization (i.e., its magnitude) should be associated with the roughness of the ocean surface. In oceanography, this condition is called sea state. Exact identification of the ocean areas where maximum polarization exists is currently in progress, and inquiry as to the sea state condition at the time of earth observation has begun. Future use of polarization analysis from earth resources satellites provides possibilities of monitoring the sea state of ocean areas not normally covered by other means.

VII. Summary

The first results of the photometry and polarimetry of the earth are given in this paper. The earth reflectance is slightly higher than expected from some astronomical data, although some authors (Ref. 3) have predicted such values. Specular reflection of sunlight from the ocean areas show large amounts of polarization. A possible correlation exists between the degree of polarization and the sea state of the ocean.

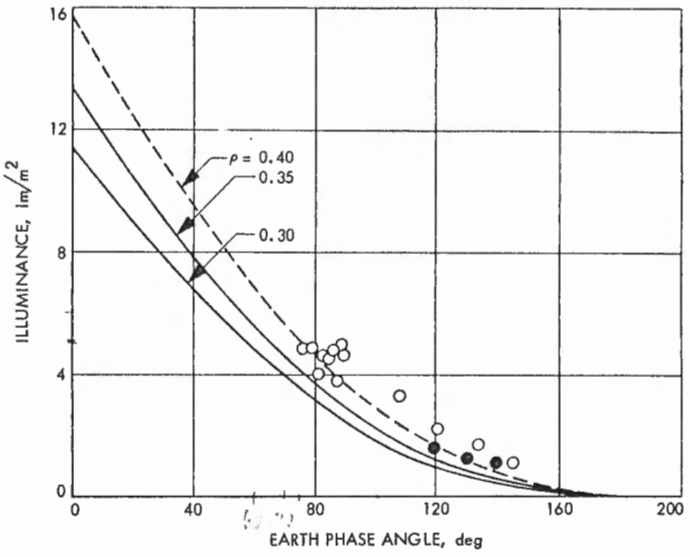

Fig. 5. Calculated average earth luminance obtained from the data presented in Fig. 5 and known angular size of earth

References

1. *Surveyor Project Final Report: Part II. Science Results,* Technical Report 32-1265. Jet Propulsion Laboratory, Pasadena, Calif., June 15, 1968.

2. De Vancouleurs, G., *Phase Curves and Albedos of Terrestrial Planets,* DDC AD-261165, June 1961 (also available as R-TR-61-26-A, Geophysics Corporation of America).

3. Danjon, A., "Albedo, Color, and Polarization of the Earth," *The Moon, Meteorites, and Comets—The Solar System,* Chapter 15. University of Chicago Press, 1962.

Colorimetric Measurements of the Solar Eclipse and Earth From *Surveyor III*

J. J. Rennilson
California Institute of Technology
Pasadena, California

I. Introduction

Of the five successful *Surveyor* missions, *Surveyor III* was perhaps the most fortuitous of all because it was treated to an event never before seen by man, that of an eclipse of the sun by his own planet. Originally such observation was not planned for; indeed the physical limitations of the television camera were such as to prevent observation of this event. Fortunately, the spacecraft landed in a crater and in the exact orientation that enabled the camera to look well above its own horizon.

The television camera on the *Surveyor* spacecraft possessed a 16-deg tilt to a horizontally landed vehicle. Thus, when *Surveyor III* landed on a slope of 14 deg, the resultant camera tilt was 23 deg with respect to the local lunar vertical. Because the camera tilt plane was oriented toward the northwest, the earth could be observed only in the wide-angle mode.

The solar eclipse began at 09:48 GMT on April 24, 1967. Shortly after the start of the eclipse, the camera was commanded to its highest elevation step, to the wide-angle mode, and to photograph two sets of pictures. Later in the *Surveyor III* mission, the camera was pointed to its upper elevation limit and was commanded to photograph the earth in its crescent phase. On each of these series, the filter wheel containing color filters (blue, green, and red) was cycled. This paper describes the colorimetric results of these observations.

II. Conditions of Exposure

The solar eclipse as seen from the moon is, of course, a lunar eclipse viewed from the earth. The earth subtends an angle of about 1.9 deg at the lunar surface, thus the inner corona is only visible shortly after the beginning of totality and shortly before its end. The motion of the moon causes an apparent motion of the sun

relative to the earth, and its path has been calculated by E. Whitaker and presented in the *Surveyor III* mission report (Ref. 1). Figures 1 and 2 are repetitions of these figures in the report and are used here for convenience.

Because the television camera did not photograph the beginning or end of totality, the only light reaching *Surveyor III* was from sunlight refracted by the earth atmosphere. Present in this light path were aerosols that acted as scattering media and thus effectively filtered out the major contribution of blue light. In the case of the earth picture series, the predominately high reflectance of the clouds with respect to the oceans greatly exceeded the dynamic exposure range of the camera; hence, an exposure was chosen so that the oceans and land areas were underexposed.

III. Camera Parameters

Two complete series of frames were taken of the solar eclipse on April 24, 1967. The first series was taken at 11:24 GMT or about 42 minutes after the start of totality and a second series at 12:01 GMT. During each series, the filter wheel was rotated and two frames through each color filter were exposed. The first series was exposed using an iris of f/4 for the blue, for the green, and for the red filter. The second series was exposed at f/5.6. The earth series was taken at 10:37 GMT on April 30, 1967, and exposed at f/5.6 in the blue, the green, and the red.

A. Color Measurement

The color filters used on *Surveyor III* were the first *Surveyor* set designed to fit the CIE (Internation Commission on Illumination) color matching functions. These functions are derived from a system of color measurements using experimental laws of color matching by human observers. Such laws state that most real colors may be visually matched by an additive combination of not more than three fixed primary colors in suitable amounts.

The remaining spectral colors not matched by the above technique require the addition of either one or two of the primary colors to the spectral color before a match to the remaining primaries is possible. The choice of the three primaries is made on the basis of independence; i.e., no primary can be matched by the addition of the two remaining primaries.

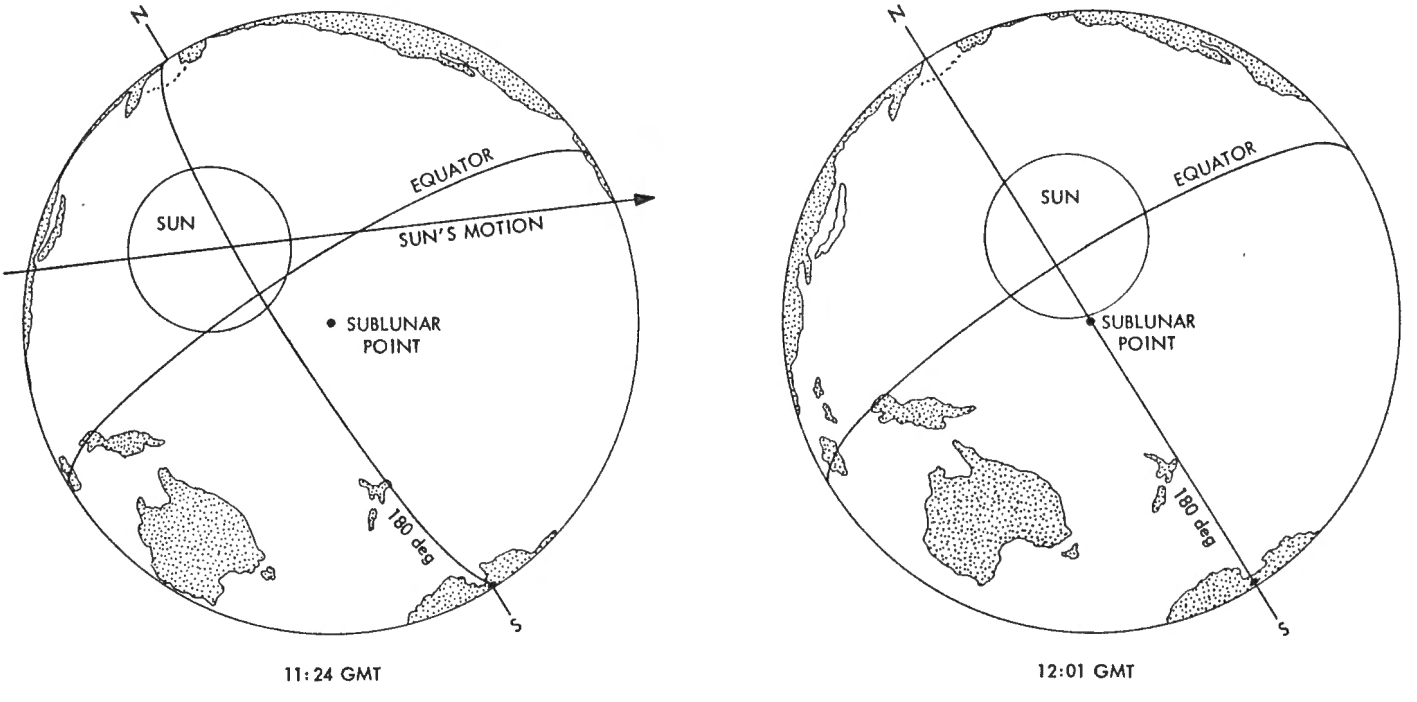

Fig. 1. Diagrams showing orientation of earth and position of sun, as seen from the moon on April 26, 1967, at 11:24 and 12:01 GMT

A color space is therefore tridimensional and may be represented by vector nomenclature. In Fig. 3, the real primaries formed from spectrum colors are base vectors **R**, **G**, and **B**. Each arbitrary color **Q** is then represented as a vector whose scalar magnitude is proportional to its luminance. The components of **Q** on the base vectors **R**, **G**, and **B** are *R*, *G*, and *B*; they are called tristimulus values. If a plane now cuts these base vectors at some angle, the vectors of all visual spectrum colors will trace an intersectional locus shown by the horseshoe-shaped curve in Fig. 3. Examination of a real color vector in a portion of the intersectional curve will show that the components are not all positive quantities, since the coordinates of these spectrum colors lie outside the triangle formed by the three primaries.

Since color space is a mathematical concept, it may be treated by the rules of vector transformation. Three new base vectors **X**, **Y**, and **Z** may then be formed by appropriate transformation from the original three **R**, **G**, and **B** vectors. Although such a transformation may take any mathematical form, one particular transformation was agreed upon in 1931 by an international body. It in this system of color measurement that is used in the *Surveyor III* data reduction.

The two main objectives used in establishing this specific transformation were:

(1) That the components (tristimulus values) of any real color vector on its base vectors **X**, **Y**, and **Z** always be positive quantities.

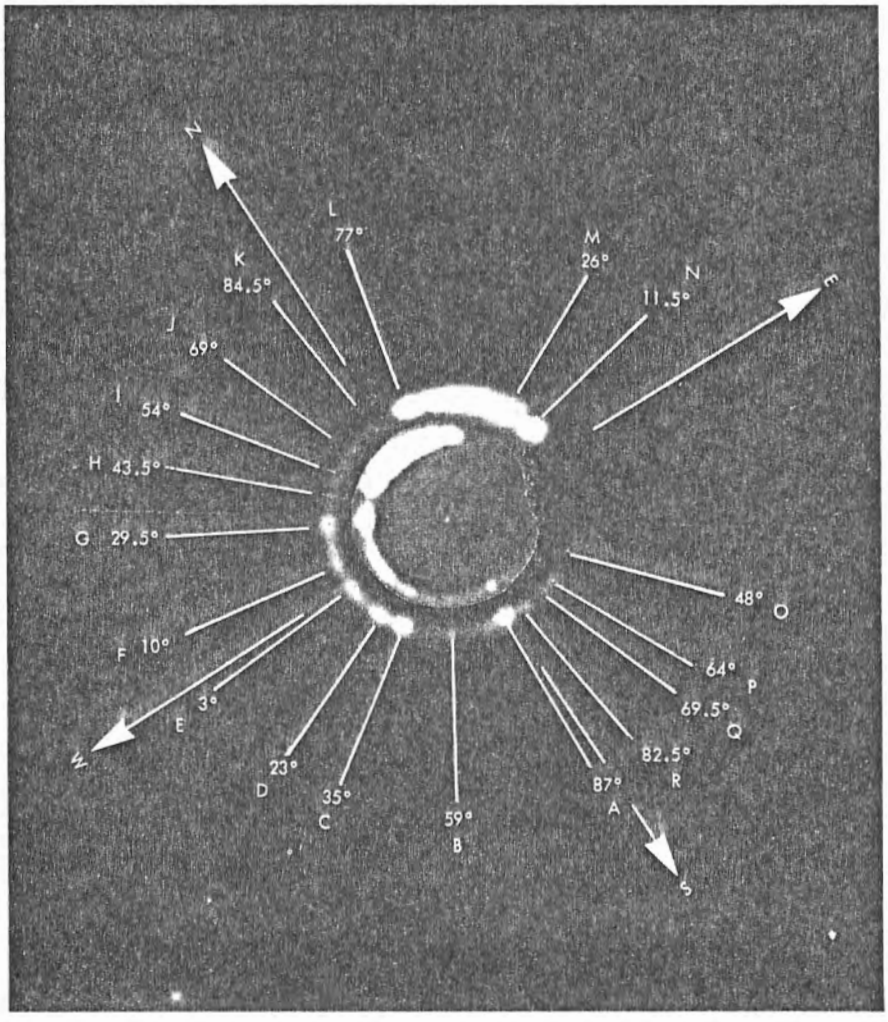

Fig. 2. Superimposed *Surveyor III* pictures (first and second series) showing distribution of light in refraction halo of earth (eighteen beads are identified by letters)

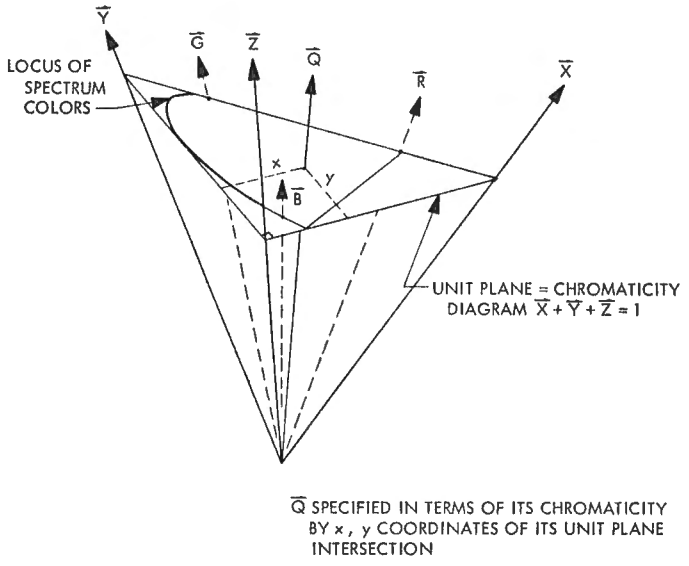

Fig. 3. Color space in vector notation

(2) That the Y component only be proportional to the luminance or reflectance of the color.

Thus, the determination of the tristimulus values X, Y, and Z of a given color specifies not only its color or chromaticity, but its luminance or reflectance as well.

When the components (tristimulus values) of each of the spectrum colors from an equal-energy spectrum (all wavelengths possessing equal radiant energy) are plotted at their corresponding wavelengths, the spectral response curves shown in Fig. 4 result. In the limiting case, the three components comprise three functions labeled $\bar{x}$, $\bar{y}$, and $\bar{z}$. These are often called color matching functions as they represent the quantities of the X, Y, and Z primaries required to match a constant radiant energy at each spectral wavelength. If a detector possesses the spectral responses corresponding to these color matching functions $\bar{x}$, $\bar{y}$, and $\bar{z}$, then its signal will be proportional to the tristimulus values X, Y, and Z of the measured color.

The *Surveyor III* camera was fitted with color filters to approximate the color matching functions $\bar{x}$, $\bar{y}$, and $\bar{z}$. The filter selection consisted of choosing glasses matching the spectral response of the vidicon, lens, and mirror combination (Fig. 5) for the best fit to the color matching functions. The two physical limitations imposed on this fit were: (1) that the total glass thicknesses be limited to 3 mm and (2) that the minimum thickness of any element of the filter be 1 mm.

A computer program using the method of Davies and Wyszecki (Ref. 2) is used to choose the glasses and then

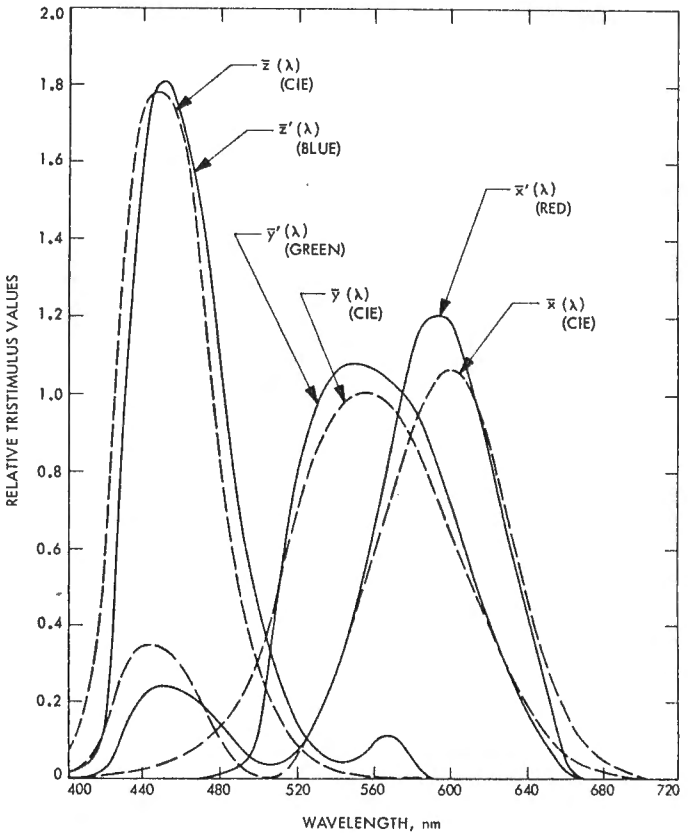

Fig. 4. Camera-filter spectral response functions of the *Surveyor III* camera, compared with CIE color-matching functions

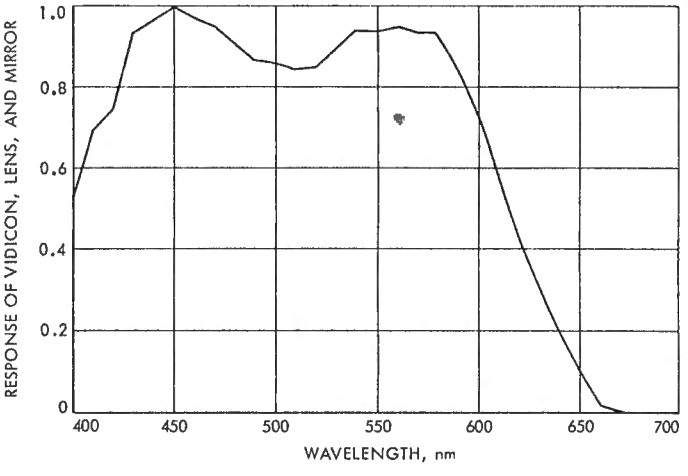

Fig. 5. Spectral response curve of the *Surveyor III* television camera at clear position

obtain the best fit to the CIE functions. The first maxima of the $\bar{x}$ function is simulated by using a reduced value of the $\bar{z}$ function added to the remaining $\bar{x}$ function. This simulation is standard practice in colorimetry since double-peaked filters are difficult to obtain. The resultant

best fit to the CIE function of the camera-filter combinations are shown by the dotted curves in Fig. 4. In addition, a light deposit of Inconel is applied to two of the three filters in order to equate the camera signals when measuring a neutral gray under sunlight.

B. Camera Measurement

The three camera signals as recorded on the ground do not automatically yield the tristimulus values. The degree of fit to the color matching functions, as well as the differences in the camera signals, accounts for this disparity. The tristimulus values are related to the camera signals by the following equations:

$$X = k_{x1}R_x + k_{x2}R_x \tag{1a}$$

$$Y = k_yR_y \tag{1b}$$

$$Z = k_zR_z \tag{1c}$$

where R_x, R_y, and R_z are the camera signals corrected for nonlinear response, and k_{x1}, k_{x2}, k_y, and k_z are proportionality factors. These factors are determined experimentally by measuring camera signals derived from known color stimuli. The proportionality factors are then calculated to minimize the sum of the squares of the differences between the true and measured tristimulus values.

The *Surveyor III* camera observed a nine filter and light source combination stimulus during preflight calibration. The proportionality factors thus determined were $k_{x1} = 3.820$, $k_{x2} = 15.412$, $k_y = 19.590$, and $k_z = 12.34$. A more complete explanation of proportionality factors and camera measurement is found in Ref. 3.

C. Colorimetric Accuracy

Color measurements are often described by coordinates of the intersectional point in the unit plane of the color vector. This unit plane, called the chromaticity diagram because it includes only the color and not the luminance values, is shown in Fig. 3. The coordinates are related to the tristimulus values by the equations

$$x = \frac{X}{X + Y + Z} \tag{2a}$$

$$y = \frac{Y}{X + Y + Z} \tag{2b}$$

Around the chromaticity of extraterrestrial sunlight ($x = 0.318$ and $y = 0.330$), the eye can detect color differences of about ± 0.001 in x and y under good observing conditions. The *Surveyor III* camera yielded proportionality factors that enabled chromaticities near the illuminant color to be measured with an accuracy of ± 0.006 in x and y.

The accuracy given above depends on three main factors:

(1) The degree of fit to the CIE color matching functions.

(2) The linearity of the camera to different luminance levels through each filter.

(3) The temperature and signal stability of the overall camera system.

Of these three effects, the latter two are the most important.

During preflight calibration, the camera observes a uniform light source of spectral radiance approximating the sun outside our atmosphere. This source completely fills the camera field-of-view in the narrow-angle mode. The luminance of the source may be varied continuously. The camera signals from such a source may be plotted against the source luminance to yield a light transfer characteristic curve. When such calibration is repeated for each color filter in the camera, light transfer characteristics result for the eclipse image area, as shown in Fig. 6. Vidicon shading defined as variation in sensitivity across the image format, is also recorded with this source. As is seen in the figure, the filter transmissions are not equal for a source approximating the sun.

The nonlinear transfer characteristics give rise to an interesting effect in the chromaticity diagram. For example, in Fig. 6, if the camera signals through the red and green filters are on the semilinear portion of the transfer characteristic, but the blue is close to the toe, then the uncertainty in the blue signal will be reflected in its tristimulus value. Furthermore, if the chromaticities determined from Eqs. (1) and (2) are calculated, keeping the blue R_z and the green R_y signals constant and allowing the uncertainty of the red R_x signal to vary, then a series of dots results on the chromaticity diagram. Figure 7 shows these dots lying along line 1 that, if extended, intersects the end of the diagram at $x = 1.0$ and $y = 0.0$ (the intersection of the X primary and the chromaticity diagram). Similarly, other lines are formed

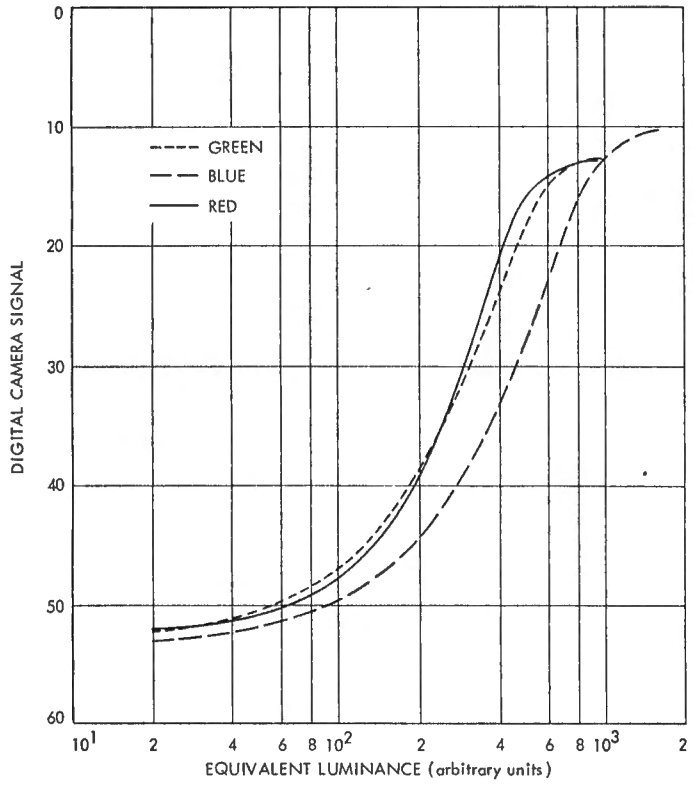

Fig. 6. Light transfer characteristics of eclipse image area through three filters

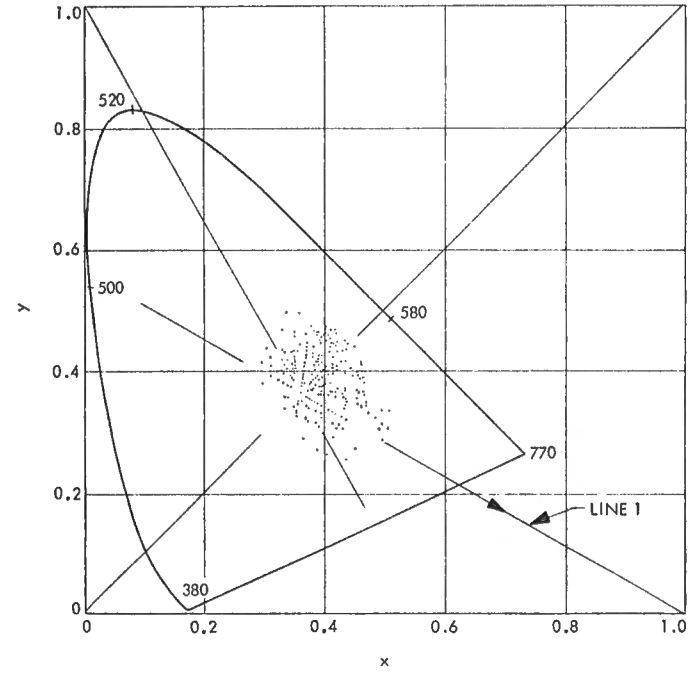

Fig. 7. Chromaticity errors resulting from uncertainty in one or two camera signals

when either one or two of the three camera signals are varied and the other(s) held constant. Thus a star-like appearance occurs in the diagram and is very symptomatic of nonlinearity errors in the respective camera signals. Such a diagram was first seen in the early reduction of the *Surveyor III* eclipse frames. The cause of this erroneous data was not determined until after the completion of the *Surveyor* missions; this cause will be explained in the next section.

IV. Data Reduction

A. Frame Digitization

The data reduction of the eclipse frames involved digital conversion of the analog video tapes. The video signal was digitized to six bits (0–63). The transfer characteristics shown in Fig. 6 were used to convert the digital values to equivalent luminances, and Eqs. (1) and (2) were then used to compute the chromaticities. The image was broken into 600 lines by 684 elements. The greater width of the frame is a function of the communications bandwidth. Each picture element (called a pixel) thus yielded a chromaticity. The chromaticities were then plotted on the diagram and gave a result similar to Fig. 7. The search for the error was then directed along other lines.

B. Image Spread and Expected Image Size

During the *Surveyor* program, it was suspected that image bleed or spread of point images would occur. This effect was observed in early tests using stellar images. The magnitude of this effect was not measured, at any time, on the actual flight vidicons. It thus remained the province of post-mission analysis to quantitatively describe the spread.

A special test was devised using a rear-illuminated slit and an extra flight-type camera. The slit dimensions were chosen so that its width subtended less than one-third of a picture element under ideal conditions of image formation. The measurement of the spread of this slit was thus a combination of the lens line spread function and a spread function associated with the vidicon.

Figure 8 shows what happens when the luminance behind the slit is increased. The image width is measured at one-tenth of its peak value. Comparison with the light transfer characteristic curve shows that an image spread effect begins to occur when the signal is 85% of the saturation level. From that point on the

spread follows the equation

$$x = -13.61 + 5.05 \ (\log L)$$

where x is the number of picture elements and L is the source luminance. Examination of stellar images that have been computer processed indicate a slightly larger size than that given in Fig. 8.

The expected image size of the illuminated portion of the eclipse is found from the astronomical data. If the effective optical atmosphere of the earth is 65 km in height, then the width of the image (atmosphere thickness) is less than one-third of a picture element for the solar eclipse. For the earth, the image is only 50 elements in diameter. It is therefore necessary to assume the conditions of image spread.

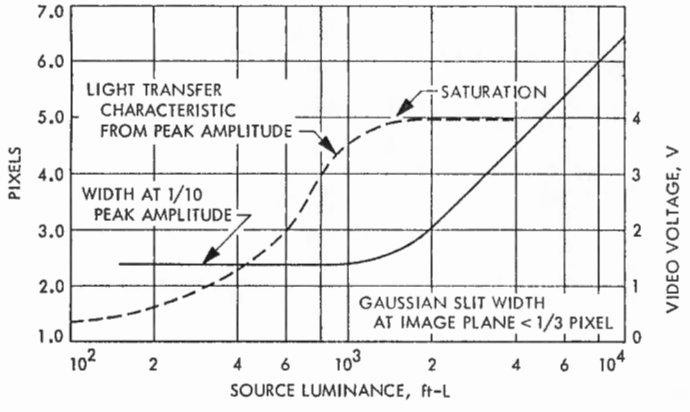

Fig. 8. Plot of image spread of an unresolved slit image as saturation is approached and exceeded

Cross sections of the first solar eclipse picture through the bright saturated cap and then through an area at approximately 43.5 deg N latitude is shown in Figs. 9 and 10, respectively. Both sections of each figure are plotted using uncorrected raw video and the corresponding equivalent luminances. In Fig. 9, the center of the cap reaches saturation. In Fig. 10, there still exists a spread of the image even in the presence of a nonsaturated video signal. This may be caused by the light scattering from lunar material present on the camera mirror.

In view of the unresolved differences, it thus appeared that the total video signal for an unresolved image would be equal to the integral

$$s = \int L \, dx \simeq \Sigma \, L \, \Delta x$$

where L and x have the same meaning as given previously.

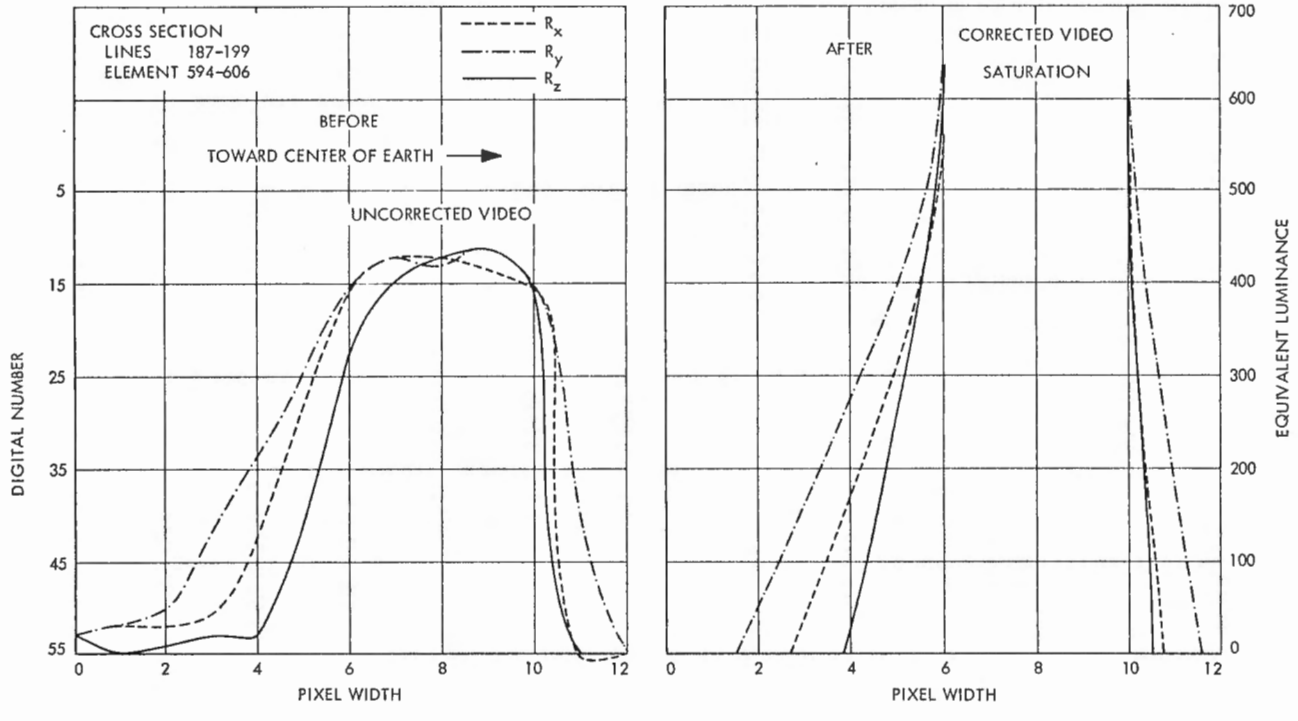

Fig. 9. Signal cross section through bright saturated cap (before and after correction for nonlinear transfer characteristics)

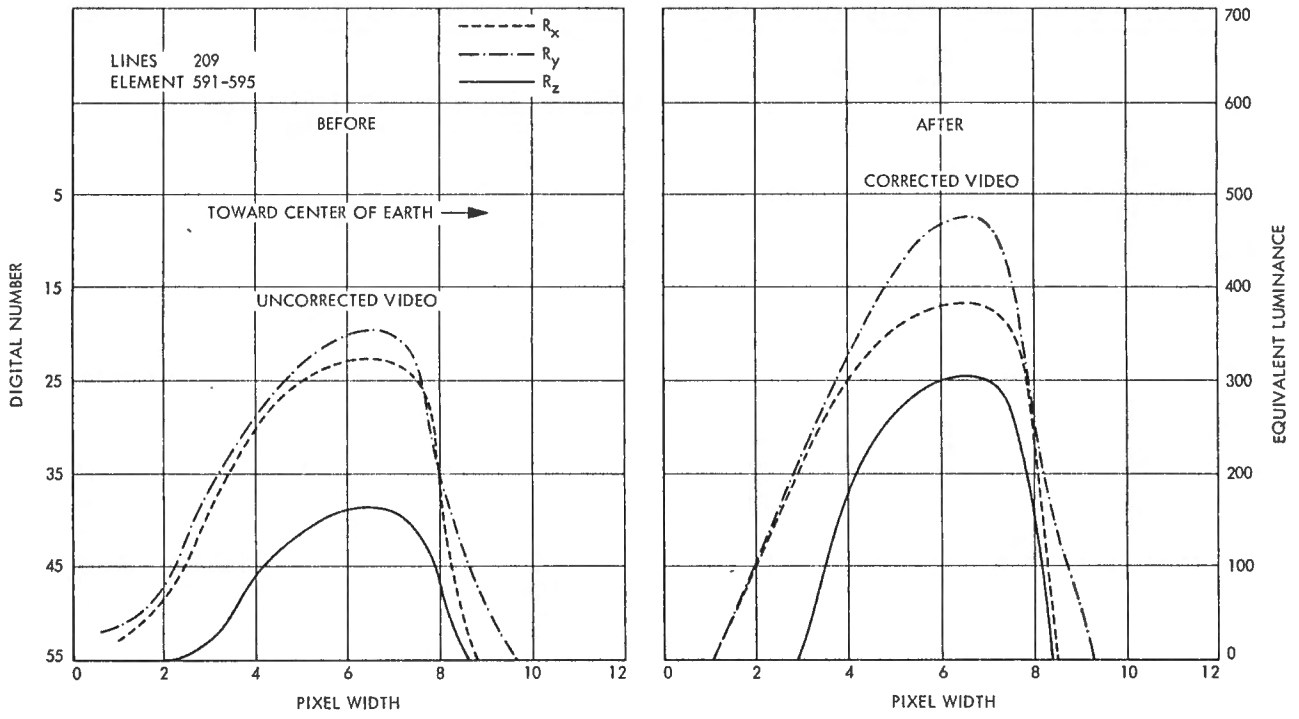

Fig. 10. Signal cross section at 43.5 deg N latitude (both before and after correction for nonlinear transfer characteristics)

C. Results

Using the above assumption, the eclipse frames chromaticity coordinates were computed for approximately every 10 deg in earth latitude. The results, numbering 35, are given in Table 1; corresponding points are shown on the chromaticity diagram of Fig. 11. Two points marked with crosses and labeled G denote the chromaticity measurements of bead G from the second series of eclipse pictures. Remaining portions of the image were sufficiently underexposed to cause large uncertainties in the measurements. For comparison, the chromaticity locus of a full radiator, radiating in accordance with Planck's law, is also plotted in Fig. 11. Four isotemperature lines at 3000, 3500, 4444, and 5000°K are likewise shown crossing the locus. The chromaticities in general are grouped close to these isotemperature lines.

The location (in relation to latitude) of the color measurements on a black and white frame is shown in Fig. 12. The prominent bead G is also marked on this figure.

The measurements of the earth, as was previously mentioned, were underexposed in the cloud-free areas. The average chromaticity of the clouds is also plotted in Fig. 11 and given in Table 1.

V. Conclusions

The colors of the eclipse as measured by *Surveyor III* show a fair degree of blue attenuation as the sunlight is refracted through the atmosphere. Calculations could be made to determine the expected chromaticities assuming various aerosols, but this effort was considered beyond the scope of this paper. It is sufficient to state that the color variations are undoubtedly caused by the degree of scattering in the cloudy vs clear areas, as well as particulate material in the aerosols. The colors, especially in the clear areas of the atmosphere, also increase in purity as the angular separation increases between these areas and the sun. This change is most apparent in bead G.*

The average earth chromaticity, determined largely by cloud cover, agrees well with the chromaticity of extraterrestrial sunlight. The clouds are thus fairly neutral reflectors in the visible spectral region. Most all land areas were cloud covered at the time of observation, and the clear ocean areas were sufficiently underexposed to render that data inaccurate.

*No detection of the solar corona was noted in the eclipse frames. Exposures for the corona, 1–2 earth radii distant, would have rendered the refracted sunlight unmeasurable.

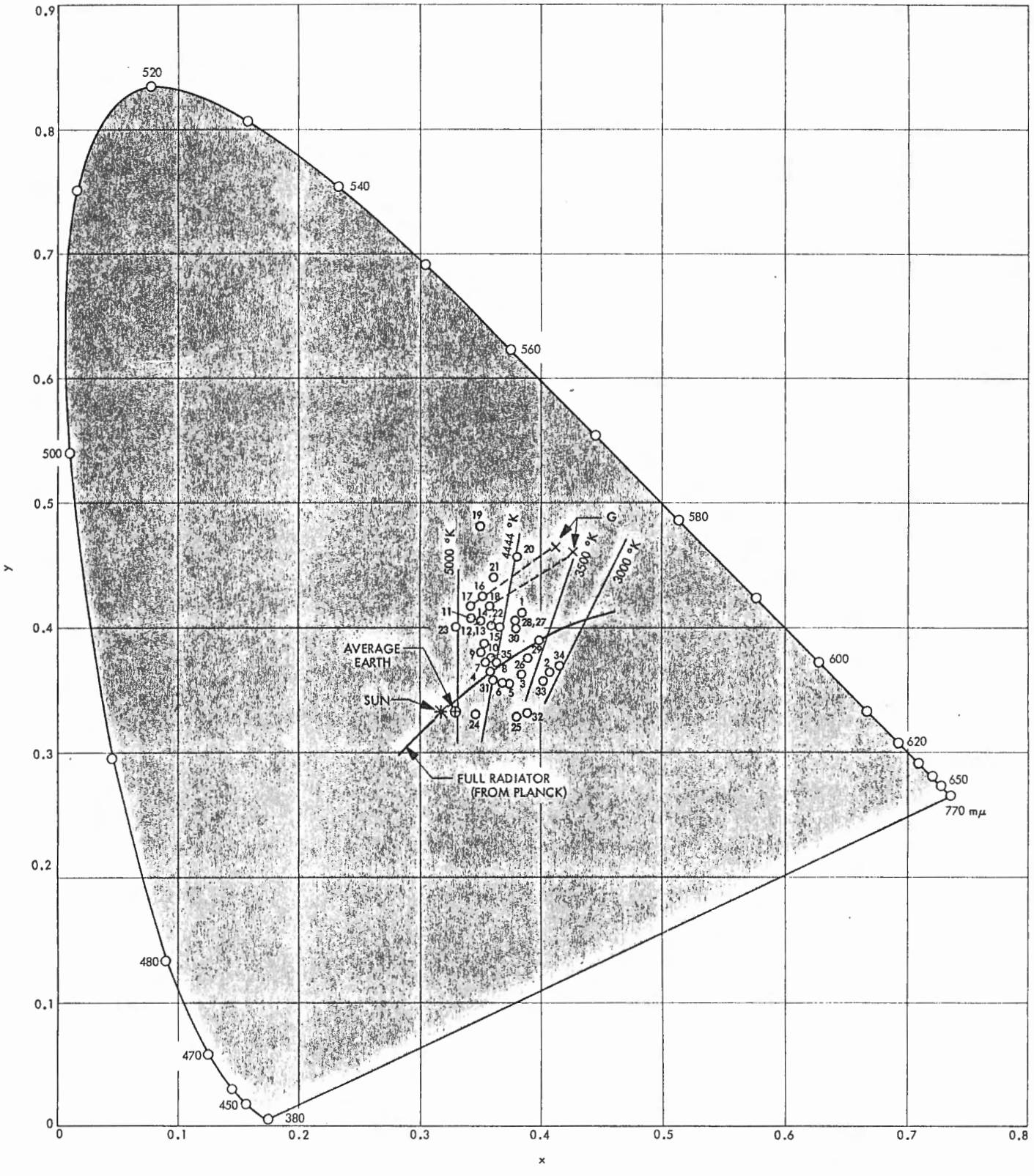

Fig. 11. Plot of the chromaticities of the eclipse and earth cloud cover based on 1931 CIE chromaticity diagram

Table 1. Eclipse frames chromaticity coordinates

Position	x	y	Position	x	y	Position	x	y
1	0.386	0.411	14	0.361	0.399	27	0.378	0.403
2	0.408	0.363	15	0.365	0.400	28	0.380	0.404
3	0.385	0.360	16	0.353	0.425	29	0.399	0.388
4	0.358	0.364	17	0.343	0.416	30	0.379	0.398
5	0.375	0.352	18	0.359	0.417	31	0.361	0.356
6	0.370	0.354	19	0.352	0.481	32	0.388	0.332
7	0.356	0.371	20	0.381	0.457	33	0.403	0.354
8	0.364	0.370	21	0.361	0.440	34	0.416	0.368
9	0.351	0.379	22	0.361	0.398	35	0.360	0.373
10	0.354	0.385	23	0.330	0.399	G[a]	0.429	0.460
11	0.344	0.407	24	0.347	0.328	G	0.414	0.467
12	0.352	0.403	25	0.372	0.327	⊕[b]	0.325	0.330
13	0.351	0.404	26	0.391	0.374			

[a]Chromaticity measurements of bead G.

[b]Average chromaticity of earth clouds.

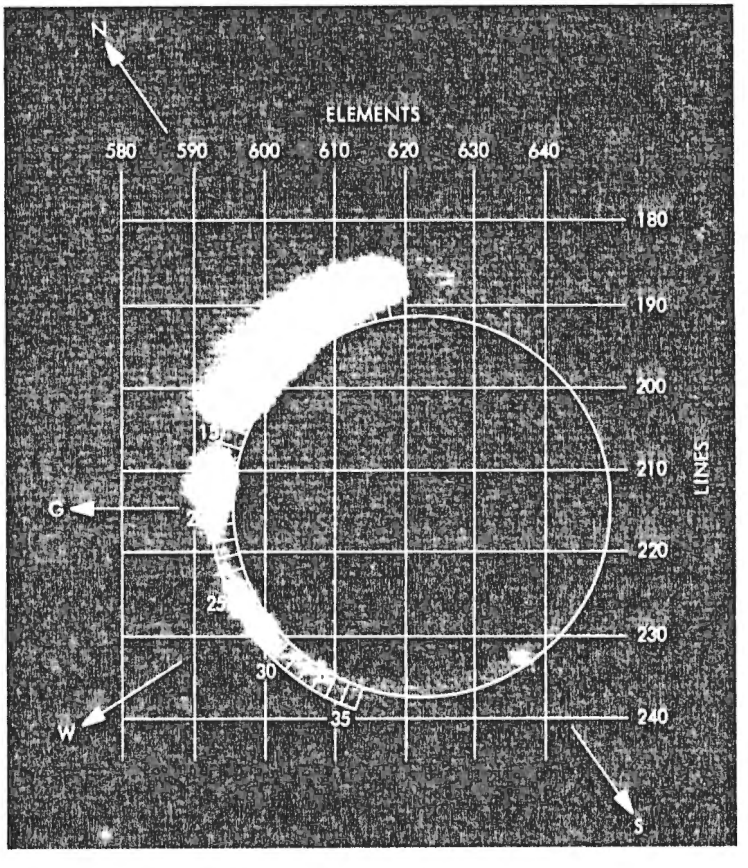

Fig. 12. A frame through green filter of first series of eclipse pictures on April 24, 1967, at 11:23:01 GMT

References

1. *Surveyor III Mission Report: Part II. Scientific Results*, Technical Report 32-1177. Jet Propulsion Laboratory, Pasadena, Calif., June 1, 1967.

2. Davies, W. E., and Wyszecki, G., "Physical Approximation of Color-Mixture-Functions," *J. Opt. Soc. Am.*, Vol. 52, No. 6, pp. 679–685, June 1962.

3. Rennilson, J. J., "A Television Colorimeter for Lunar Exploration," in *Proceedings of the 8th International Colour Meeting, Lucerne, Switzerland.* Centre d' Information de la Couleur, 23 Rue Notre-Dame-des-Victoire, Paris, France, pp. 498–506, June 1965.

NASA — JPL — Coml., L.A., Calif.